ORDERED STRUCTURES IN NUCLEAR AND ATOMIC PHYSICS*

R.W. HASSE

Plasma Physics Division, Gesellschaft für Schwerionenforschung GSI
D-64220 Darmstadt, Germany
E-mail: UL29DAGSI3.GSI.DE

(Received August 28, 1993)

With the help of molecular dynamics computer simulations we study the equilibrium configurations and the volume and surface energies at low temperature of large systems of classical interacting particles either under the influence of their mutual long range Coulomb forces and a radial harmonic external confining force or of the short range Lennard-Jones potential. The former is a model for charged particles in ion traps and the latter for clusters. For the Coulomb plus harmonic force, the particles arrange in concentric spherical shells with hexagonal structures on the surfaces. The closed shell particle numbers agree well with those of multilayer icosahedra (mli). A Madelung (excess) energy of -0.8926 is extracted which is larger than the bcc value. The results are compared with those obtained by a simple onion shell model. For the Lennard–Jones force we employ various initial configurations like multilayer icosahedra or hexagonal closed packed (hcp) spheres. Cohesive (volume) and surface energies per particle are extracted and compared to the energies of scaled mli quasicrystals and of spherical scaled crystals with N up to 36 000. It is shown that relaxed mli are the dominant structures for $N < 5\,000$ and hcp spheres for larger particle numbers. For $N < 22\,000$, hcp crystals have about the same closed shell numbers as mli quasicrystals but smaller ones for $N > 22\,000$. The same magic numbers are obtained with other short range Mie potentials. The stable Argon cluster configurations calculated with a realistic pair potential are mli for $N < 750$, hcp for $750 < N < 9300$ and face centered cubic (fcc) for $N > 9300$.

PACS numbers: 52.25. -b, 52.65. +z, 36.40. +d

---

* Presented at the XXIII Mazurian Lakes Summer School on Nuclear Physics, Piaski, Poland, August 18–28, 1993.

1. Introduction

A cooled gas liquifies and a cooled liquid crystallizes. This applies to all kinds of matter with equations of state similar to the one of an ideal gas. In particular, a system of charged particles under the influence of their mutual Coulomb repulsion and of a neutralizing background yields so-called Wigner or Coulomb crystals [1–3] The same holds for a system of charged particles bound by an external confining force, for instance of light charged ions in electromagnetic traps [4–6]. Here the structures of systems of a few (one to ten, or even up to a few thousand) light ions in Penning or Paul traps of various, even toroidal [7], shapes have been studied experimentally in detail with the help of laser cooling. Typical interparticle distances are of the order of a few micrometers in contrast to ordinary crystals with distances of a few Ångströms. Two-dimensional Wigner solids can also be produced with an electron plasma at solid-state heterojunctions [8]. However, whereas in infinite systems there exists a sharp phase transition between the liquid and crystalline states, this is washed out in finite systems.

In this connection, the properties of ions confined in an external field has become of recent interest with the advent of the low temperatures attained in storage rings with electron cooling, especially for heavy ions [9–11], and Schiffer and Kienle [12] have suggested that an heavy ion beam might attain an ordered liquid or crystal state.

In this lecture we are concerned with the structure and energetics of a system of confined ions under the influence of a radial focusing force and under either the long range Coulomb or the short range Lennard-Jones or similar force. What is the (quasi-) crystalline structure of such an ensemble of many charges? Are there transitions from one kind of (quasi-) crystalline structure to another? How large is the volume (or Madelung or excess or cohesive) energy, *i.e.* the energy per particle of an infinite system, and can one extract surface energy coefficients? Is there a classical shell energy and what are the magic particle numbers at which the structures are most stable?

The strongly correlated infinite one-component plasma (OCP) crystallizes in an bcc lattice if the plasma parameter, *i.e.* the ratio of Coulomb to thermal energy, reaches the value [3] $\Gamma \approx 171$. Finite systems, on the other hand, exhibit hexagonal structures on the surfaces [13, 14], however imperfect due to the incompatibility between a perfect lattice and a curved surface and due to the incommensurability of two adjacent shells. A change of structure from the plane hexagonal into the bcc one occurs only if the dimensions of the system become as large as about 100 interparticle distances [15].

2. Coulomb plus harmonic forces

In order to study large but finite Coulomb systems we extend the calculations on small systems by Rafac *et al.* [16] and employ the molecular dynamics (MD) technique to solve the classical equations of motion under the external harmonic confining force

$$\boldsymbol{F}^i_{\text{conf}} = -K\boldsymbol{r}_i,$$

and the Coulomb force,

$$\boldsymbol{F}^i_{\text{Coul}} = -q^2 \sum_{j\neq i} \frac{\boldsymbol{r}_i - \boldsymbol{r}_j}{|\boldsymbol{r}_i - \boldsymbol{r}_j|^3}.$$

The initial momenta are chosen at random as to give an initial kinetic energy corresponding to $\Gamma \approx 1$ and the initial coordinates of N ions usually are chosen as those of the (N–1)-ion system with one ion added at random. The system then is followed in time thereby cooling by reducing the momenta until thermal equilibrium has been reached; for details see Ref. [14]. In this chapter distances are measured in units of the Wigner-Seitz radius $a_{\text{WS}} = (q^2/K)^{1/3}$ and energies in units of q^2/a_{WS}. The total energy, *i.e.* the sum of confining and Coulomb energies per particle, then reads

$$\varepsilon = \frac{1}{2N}\sum_{i=1}^{N} \boldsymbol{r}_i^2, + \frac{1}{N}\sum_i \sum_{j<i} |\boldsymbol{r}_i - \boldsymbol{r}_j|^{-1}$$

and the excess energy is defined by subtracting the homogeneous value of $\overline{\varepsilon} = \frac{9}{10}N^{2/3}$.

TABLE I

Structures, rms radii and excess energies of closed shell N-particle systems.

N	Structure	R_{rms}	$\varepsilon_{\text{excess}}$
12	12	1.6002	-0.87663
60	48+12	2.9335	-0.88498
146	93+41+12	4.0054	-0.88745
308	163+93+42+10	5.7404	-0.88919
561	255+161+93+42+10	6.3418	-0.88994
899	356+247+154+92+38+12	7.4361	-0.89059
1414	491+365+244+163+94+44+13	8.6600	-0.89124
2057	641+491+363+257+158+93+44+10	9.8209	-0.89132
2837	805+634+480+356+246+173+*143**	10.9384	-0.89172
3871	992+801+639+*1439**	12.1379	-0.8915†

* The remaining shells cannot be resolved

† At small temperature

The resulting magic numbers are listed in Table I where the excess energy is minimal as compared to the neighbouring particle numbers. The excess energy is shown in Fig. 1. For systems with $N < 64$, there are strong shell effects in the excess energy with peaks and minima if a new shell opens, in particular the transitions at $N = 12, 60, 146$. One notes that the smaller magic numbers are even as compared to those of the mli because the center particle is always missing. In particular, the second shell starts at $N = 13$, the third one at $N = 61$, and the next ones at or around $N = 147$, 309, 565, 900, 1400, 2100, respectively.

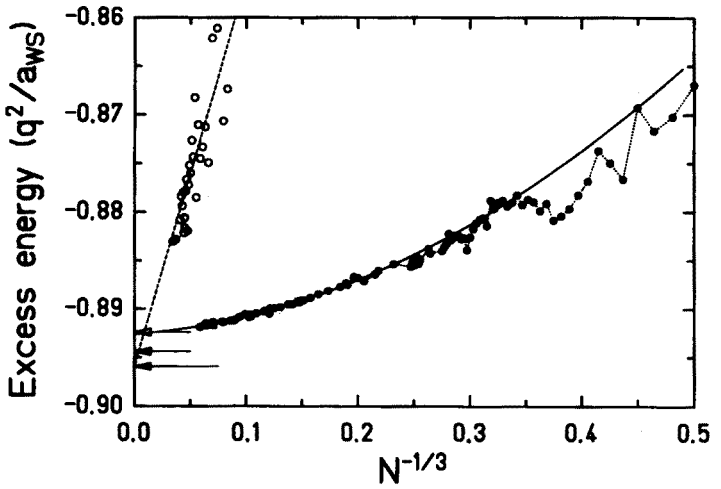

Fig. 1. Excess (Madelung) energy of Coulomb quasicrystals. The dots are MD data and the full line is the best fit. The open arrow points to the asymptotic value and the full arrow to the Madelung energy of the infinite bcc OCP. Open circles are results of spherical bcc matter together with a fit (dashed line).

These closed shell particle numbers are compatible with the magic numbers of Mackay's multilayer icosahedra (mli) [17],

$$N = (2M + 1)\left[\tfrac{5}{3}M(M + 1) + 1\right], \tag{1}$$

notably $N = 13, 55, 147, 309, 561, 923, \ldots$ which have been verified experimentally as closed shell particle numbers in metal clusters, see *e.g.*

Refs. [18, 19]. The subshell numbers are given by $10N^2 + 2 = 12, 42, 92, 162, 242, \ldots$ They are thus more general in the sense that they not only are identical to those of stacked cuboctahedra but also show up in Coulomb systems. Due to the long range nature of the Coulomb force, Coulomb quasicrystals tend to be as spherical as possible. This is not in contradiction to the edged nature of the mli because here the plane surfaces of the mli become curved.

An infinite Coulomb system can take advantage of all long range interactions in order to arrange in an bcc lattice and to minimize the Madelung energy by summing up all long range contributions. A finite system, on the other hand, can explore only the short and intermediate range parts of the Coulomb interaction. It is well known that systems with short range interactions arrange in fcc or hcp lattices with coordinations (the number of almost equal nearest neighbour distances) of 12 but with higher Madelung energies. A finite Coulomb system, hence, will arrange in such a way as to maximize the coordination *i.e.* to achieve the maximum possible number of equilateral triangles. In Fig. 2 is shown the front hemisphere of the outer shell of the 5000-particle system. Here the overall hexagonal structure is well pronounced, however with dislocations and pentagonal point defects. The particles in the next inner shell most often sit below the line connecting two particles rather than below the center of the triangle.

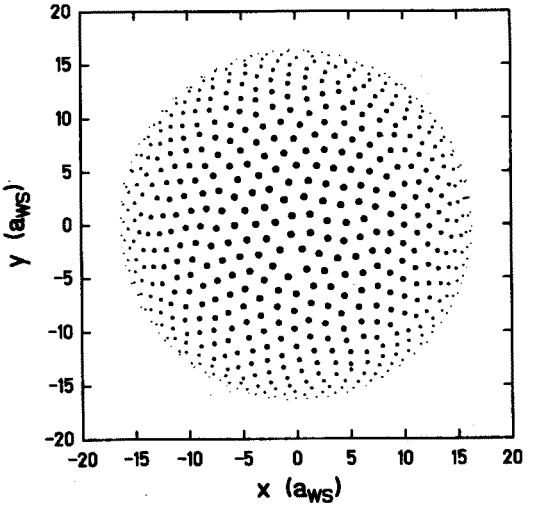

Fig. 2. The front hemisphere of the outer shell of the 5000 ion system. Note the haxagonal structure with approximately equilateral triangles and the point defect below the center.

A fit for $N > 300$ gives

$$\varepsilon_{\mathrm{MD}} = -0.8926 \pm 0.0001 + 0.0088 N^{-1/3} + 0.096 N^{-2/3}$$

with an asymptotic Madelung energy of -0.8926 which is higher than the one of the infinite bcc OCP of -0.895929, thus indicating that even at very large particle numbers the hexagonal surface structure is still dominating over the bcc structure. This is due to the small surface energy of the hexagonal lattice on the curved surfaces. The surface energy extracted from the MD data is the average over the whole surface and also includes relaxation and reconstruction of the surface that minimize the total energy. To evaluate the order of magnitude of surface relaxation we calculated the excess energies of unrelaxed spherical fragments containing up to 25 000 particles, sliced out of infinite ideal bcc matter with the same density, see the open circles in Fig. 1. Extrapolation of these data to the bcc Madelung energy (dashed line) gives a surface energy coefficient of ≈ 0.4. It crosses the fit of the MD data at $N \approx 4 \times 10^6$. This number of particles at which the infinite bcc lattice takes over energetically is compatible with the estimate of Dubin [15].

In order to explain the results of the computer simulations we compare them with those of an onion shell model, where the quasicrystals are supposed to consist of M homogeneously charged shells of radius R_ν and number of particles N_ν with the constraint $\sum_\nu N_\nu = N$. The Coulomb and confining energies then become

$$\varepsilon_{\mathrm{Coul}} = \frac{1}{N}\left[\sum_{\nu=1}^{M} \frac{N_\nu}{R_\nu}\left(\frac{1}{2}N_\nu + \sum_{\nu<\mu} N_\mu\right)\right],$$

$$\varepsilon_{\mathrm{conf}} = \frac{1}{2N}\sum_\nu N_\nu R_\nu^2.$$

This is corrected for the energy per particle of the plane hexagonal lattice [20, 15],

$$\varepsilon_{\mathrm{Mad}}^{\mathrm{p\text{-}hex}} = -\alpha/\sqrt{f},$$

where $\alpha = 1.960515789$ and f is the unit area of an ion. With the geometrical value of $f = a^2\sqrt{3}/2$, where $a = (16\pi/9)^{1/3}$ is the minimum distance, it takes on the value $\varepsilon_{\mathrm{Mad}}^{\mathrm{p\text{-}hex}} = -1.187397$. Minimization of the total energy with respect to the radii yields

$$R_\nu^3 = \frac{1}{2}N_\nu + \sum_{\mu<\nu} N_\mu, \tag{2}$$

which, in turn gives the total energy per particle

$$\varepsilon_{\text{total}} = \frac{3}{2N} \sum_{\nu} N_\nu R_\nu^2 + \varepsilon_{\text{Mad}}^{\text{p-hex}} .$$

Demanding that the area of a given shell is occupied by N_ν areas of equilateral triangles of sides a, thus also allowing for noninteger particle numbers N, N_ν,

$$4\pi R_\nu^2 = \frac{4\pi}{3d} N_\nu + \frac{5}{24} a^2 \qquad (\nu > 0) , \tag{3}$$

Eqs (2), (3) are solved iteratively with initial values $N_0 = R_0 = 0$. The excess energies without $\varepsilon_{\text{Mad}}^{\text{p-hex}}$-corrections, of course, would be positive, *i.e.* higher than the true minimum of the homogeneous system. The agreement of the shell model results with the MD results is rather good even for the first shell. The opening of new shells is accurately predicted up to parts of a particle number, and the radii and energies are well reproduced. This yields

$$\varepsilon_{\text{Mad}}^{\text{3-hex}} = -0.894383,$$

above the bcc (-0.895929), fcc (-0.895874) and hcp (-0.895838) values but below the MD result (-0.89280) and of the sc lattice (-0.880059).

3. Short range forces

The largest magic number identified in cluster experiments is around 21 300 [19]. They are well in agreement with those obtained from purely classical geometrical packing of N particles, for instance, into mli or cuboctahedra (mlc). However, the energetical stability of large crystals and quasicrystals under short range forces has only been studied extensively by Raoult *et al.* [21]. Here icosahedral, octahedral and mono-twinned fcc, decahedral, tetrakaidecahedral, hexakaiicosahedral (hki), dodecahedral pentakaitetrakontahedral (dpk) and other truncated structures are considered.

We extend these calculations to very large particle numbers and, as an approximation to the effective two-body force in clusters, we employ the short range LJ potential,

$$V_{\text{LJ}}(r) = \varepsilon_0 \left[(r/\sigma)^{-12} - 2(r/\sigma)^{-6} \right] .$$

In this chapter we will use $\varepsilon_0 = \sigma = 1$. The energy per particle is given by

$$E_{\text{LJ}} = \frac{1}{N} \sum_{i}^{N} \sum_{j<i} V_{\text{LJ}}(|\mathbf{r}_i - \mathbf{r}_j|) . \tag{4}$$

Due to the very short range nature of the LJ force a start with initial random coordinates never yields a stable configuration. Therefore we employ mli, mlc, spheres of hexagonal closed packed (hcp), face centered (fcc) or body centered cubic (bcc) matter, or even stacked rhombic dodecahedra (srd) proposed by Kepler, see Ref. [22]. Systems with particle numbers up to $N = 6\,525$ are completely relaxed by MD and those with $2 < N < 36\,000$ are studied by uniform scaling and energy minimization. Systems with nonmagic numbers of particles were started with a magic core and the extra particles at random in the next shell; for details see Ref. [23].

TABLE II

Cohesive and surface energies and scaling factors of different Lennard-Jones crystals and of infinite mli and mlc quasicrystals.

Structure	V_{LJ}	S_{LJ}	s_0
hcp	-8.611065[1]	15.5[2]	0.971228[1]
fcc	-8.610201[1]	15.4[2]	0.971234[1]
mlc	-8.59[3]	15.6[3]	0.974[3]
hki	-8.545[4]	14.23[4]	
mli	-8.54[3]	14.18[3]	0.953[3]
dpk	-8.538[4]	14.20[4]	
bcc	-8.237292[1]	15.1[2]	0.979204[1]

[1] Analytical values
[2] From minimizing scaled large spheres
[3] Estimated from MD relaxation
[4] Lower limits extrapolated from Ref. [21]

With inverse power-law potentials scaling effects can be calculated by scaling the dimensions in Eq. (4) and minimizing with respect to the scaling parameter, $s_0 = (e_{12}/e_6)^{1/6}$ to yield the minimum energy

$$E_{LJ}^{min} = -e_6^2/e_{12}\,.$$

For infinite bcc, fcc and hcp matter, the inverse-power sums e_n are known, see [24], to give the scaling parameters and cohesive energies of Table II.

Under the LJ force, hcp matter is lowest in energy, followed by fcc and bcc matter. We repeated those scaling calculations for spheres of such matter with up to 36 000 particles in order to obtain also the surface energy coefficient in the expansion

$$E_{LJ} = V_{LJ} + S_{LJ}N^{-1/3}...$$

which are also listed in Table II. Relaxation of finite systems is achieved by solving the coupled classical equations of motion with standard MD as described above.

The resulting energies are listed in Table III and shown in Fig. 3. For small systems it can be seen that the energy of mli with the magic numbers 13, 55, 147 and 309 attains minimal values as compared to surrounding nonmagic clusters.

TABLE III

Closed shell particle numbers N of shell M and their energies of relaxed mli, mlc, hcp and fcc structures and of scaled mli, hcp and fcc.

M	N	E^{MD}_{mli}	E^{MD}_{mlc}	E^{MD}_{hcp}	E^{MD}_{fcc}	E^{scaled}_{mli}	E^{scaled}_{hcp}	E^{scaled}_{fcc}
1	13	−3.4098					−3.4098	−3.1466
2	55	−5.0772	−4.8778	−4.9114	−4.7660	−5.0373	−4.9052	−2.4041
3	147	−5.9623	−5.8121	−5.8636	−5.7888	−5.8938	−5.8576	−4.0776
4	309	−6.4959	−6.3805	−6.3907	−6.3347	−6.4102	−6.3834	−5.3022
5	561	−6.8492	−6.7595	−6.7707	−6.7522	−6.7530	−6.7621	−6.1041
6	923	−7.0994	−7.0295	−7.0490	−7.0202	−6.9965	−7.0409	−6.6062
7	1415	−7.2854	−7.2312	−7.2261	−7.2454	−7.1781	−7.2184	−6.9529
8	2057	−7.4291	−7.3875	−7.3956	−7.3831	−7.3185	−7.3880	−7.1823
9	2869	−7.5432	−7.5121	−7.5204	−7.5168	−7.4304	−7.5137	−7.3676
10	3871	−7.6361	−7.6138	−7.6257	−7.6209	−7.5216	−7.6193	−7.5085
11	5083	−7.7128	−7.6982	−7.7133	−7.7037	−7.5973	−7.7071	−7.6219
12	6525	−7.7775	−7.7696	−7.7832	−7.7808	−7.6611	−7.7774	−7.7121
13	8217					−7.7156	−7.8404	−7.7849
14	10179					−7.7628	−7.8933	−7.8515
15	12431					−7.8041	−7.9420	−7.9000
16	14993					−7.8404	−7.9807	−7.9441
17	17885					−7.8726	−8.0158	−7.9865
18	21127					−7.9013	−8.0477	−8.0238
19	24739					−7.9272	−8.0748	−8.0554
20	28741					−7.9505	−8.1003	−8.0851
21	33153						−8.1223	−8.1086

Relaxed icosahedrons are lowest in energy up to $N = 3871$, with either multilayer or stacked cuboctahedrons being much higher. In addition, since simple spherical hcp crystals always have lower energy than mlc and since even fcc crystals are lower in most of this interval of particle numbers, we exclude the possibility of the existence of large cuboctahedral clusters. Due to their bcc structure the same holds for rhombic dodecahedra.

Despite the fact that mli have a very low surface energy, the volume energy and, hence, the total energy becomes too large for large particle numbers. Around particle number of 5083, hence, there is a transition to hcp crystals which, however, have larger surface energy but lower volume energy. Similar reasoning holds for the hki and dpk. The corresponding values for the cohesive and surface energies of Table II have been obtained

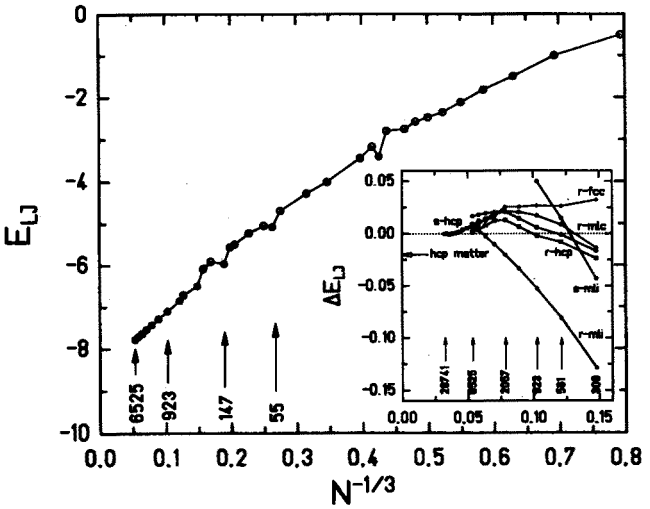

Fig. 3. Energies per particle of LJ crystals and quasicrystals. Full (open) circles are relaxed MD results with mli initial configurations at magic (nonmagic) particle numbers. In the insert are shown various energies (r: relaxed by MD, s: scaled and minimized) with the scaled-hcp average of $-8.591 + 15.035N^{-1/3}$ subtracted. The open arrow points to the hcp matter value.

by extrapolating the results of Ref. [21]. They have to be taken as lower limits. However, from Table II it can also be seen that although hki have a slightly larger surface energy than dpk, their cohesive energy is slightly less. Hki, hence becomes the more stable configuration for $N > 40\,000$.

In order to follow the magic numbers beyond $N = 6\,525$ the shell energies of scaled (but not relaxed) spherical simple cubic (sc), bcc, fcc and hcp crystals have been calculated. By subtracting the mean and smoothing we obtain the shell energies of Fig. 4. All of them exhibit characteristic shell oscillations due to the fact that there exist spherical crystalline configurations with minimum (maximum) number of surface particles at the same radius, hence with small (large) surface energies. However, for large systems sc, bcc and fcc do not show the characteristic shell spacing of Eq. (1) whereas hcp does for $N = 10\,179, 12\,431, 14\,993, 17\,885$ and $21\,127$ at the correct positions (also, at $8\,217$ there is a local minimum). The next two minima appear at $N \simeq 23\,600$ and $27\,500$ rather than at $24\,793$ and $28\,741$. Here the magic numbers were not yet identified experimentally. For larger particle numbers the shell energy becomes rather small and one expects that magic numbers cease to exist.

In order to assure that the effect of magic numbers in hcp spheres is not an artifact of the LJ force we repeated the scaling calculations with the Mie potential $r^{-4n} - 2r^{-2n}$ ($n = 3$ is the LJ potential) with $n = 1, \ldots, 4$.

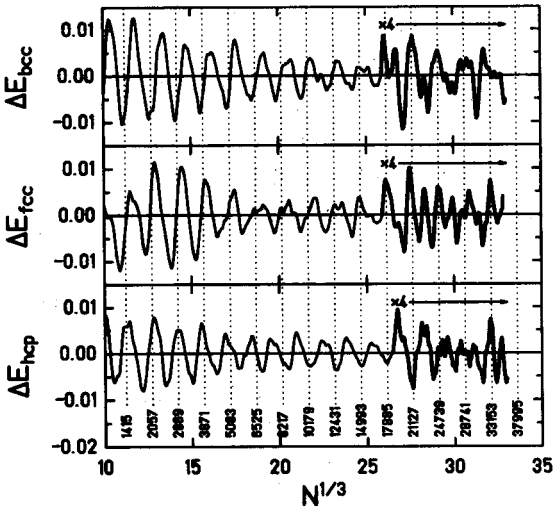

Fig. 4. Shell energies of scaled spherical LJ crystals, smoothed and the mean subtracted. The large N parts are magnified.

For the short range potentials with $n = 2, 3, 4$ we found the minima of the energy essentially at the same magic numbers as discussed above. In the long range case $n = 1$, on the other hand, the shell oscillations are very irregular and one cannot associate magic numbers. However, we cannot exclude that macroscopic structures formed of hcp matter, other than the sphere, might have even less surface energy.

Similarly, we calculated the stable configurations of Argon clusters with the realistic Argon-Argon pair potential of Ref. [25] which has an exponential and Gaussian long range tail and an e^{-1/r^2} short range cutoff. Here we found a transition from mli to hcp at particle numbers around 750 and a transition from hcp to fcc at $N \approx 9300$.

REFERENCES

[1] S.G. Brush, H.L. Sahlin, E. Teller, *J. Chem. Phys.* **45**, 2102 (1966).
[2] J.P. Hansen, *Phys. Rev.* **A8**, 3096 (1973).
[3] W. Slattery, G. Doolen, H. DeWitt, *Phys. Rev.* **A21**, 2087 (1980).
[4] F. Diedrich, E. Peik, J.M. Chen, W. Quint, H. Walther, *Phys. Rev. Lett.* **59**, 2931 (1987).
[5] D.J. Wineland, J.C. Bergquist, W.M. Itano, J.J. Bollinger, C.H. Manney, *Phys. Rev. Lett.* **59**, 2935 (1987).
[6] S.L. Gilbert, J.J. Bollinger, D.J. Wineland, *Phys. Rev. Lett.* **60**, 2022 (1988).
[7] I. Waki, S. Kassner, G. Birkl, H. Walther, *Phys. Rev. Lett.* **68**, 2007 (1992).

[8] E.Y. Andrei, G. Deville, D.C. Glattli, F.I.B. Williams, E. Paris, B. Etienne, *Phys. Rev. Lett.* **60**, 2765 (1987).
[9] J.P. Schiffer, O. Poulsen, *Europhys. Lett.* **1**, 55 (1986).
[10] A. Rahman, J.P. Schiffer, *Phys. Rev. Lett.* **57**, 1133 (1986).
[11] D. Habs, MPI Heidelberg preprint MPI H - 1987 - V 10 (1987).
[12] J.P. Schiffer, P. Kienle, *Z. Phys.* **A321**, 181 (1985).
[13] R.W. Hasse, J.P. Schiffer, *Ann. Phys.* **203**, 419 (1990).
[14] R.W. Hasse, V.V. Avilov, *Phys. Rev.* **A65**, 4506 (1991).
[15] D.H.E. Dubin, *Phys. Rev.* **A40**, 1140 (1989).
[16] R. Rafac, J.P. Schiffer, J.S. Hangst, D.H.E. Dubin, D.J. Wales, *Proc. Natl. Acad. Sci.* USA **88**, 483 (1991).
[17] A.L. Mackay, *Acta Crystallogr.* **15**, 916 (1962).
[18] H. Göhlich, T. Lange, T. Bergmann, T.P. Martin, *Phys. Rev. Lett.* **65**, 748 (1990).
[19] T.P. Martin, T. Bergmann, H.Göhlich, T. Lange, *Z. Phys.* **D19**, 25 (1991).
[20] H. Totsuji, J.-L. Barrat, *Phys. Rev. Lett.* **60**, 2484 (1988).
[21] B. Raoult, J. Farges, M.F. De Feraudy, G. Torchet, *Phil. Mag.* **B60**, 881 1989).
[22] I. Stewart, *New Scientist*, 13 July 1991, p. 29.
[23] R.W. Hasse, *Phys. Lett.* **A161**, 130 (1991).
[24] C. Kittel, *Introduction to Solid State Physics*, Wiley, New York, 5th ed. 1976, p. 80.
[25] B. Romald, A. Aziz, M.J. Slaman, *Mol. Phys.* **B58**, 679 (1986).